Density dependence in demography and dispersal generates fluctuating invasion speeds

Lauren L. Sullivan[a,1], Bingtuan Li[b], Tom E. X. Miller[c], Michael G. Neubert[d], Allison K. Shaw[a,1]

[a]Department of Ecology, Evolution and Behavior, University of Minnesota, Saint Paul, MN 55108; [b]Department of Mathematics, University of Louisville, Louisville, KY 40292; [c]Department of Ecology and Evolutionary Biology, Rice University, Houston, TX 77005; [d]Biology Department, Woods Hole Oceanographic Institution, Woods Hole, MA 02543

Author contributions: T.E.X.M., M.G.N., and A.K.S. designed research; L.L.S., T.E.X.M., M.G.N., and A.K.S. performed research; L.L.S., B.L., T.E.X.M., M.G.N., and A.K.S wrote the paper.

[1]To whom correspondence should be addressed. Email: lsulliva@umn.edu, or ashaw@umn.edu

keywords: invasion, Allee effects, density-dependent dispersal, overcompensation, pushed invasion wave

Classification: Biological Science

Abstract

Density dependence plays an important role in population regulation, and has a long history in ecology as a mechanism that can induce local density fluctuations. Yet much less is known about how these endogenous processes affect spatial population dynamics. Biological invasions occur through the combined action of population growth (demography), and movement (dispersal), making them relevant for understanding how density dependence regulates spatial spread. While classical ecological theory suggests that many invasions move at a constant speed, empirical work is illuminating the highly variable nature of biological invasions, which can lead to non-constant spreading speeds. Here, we explore endogenous density dependence as a mechanism for inducing variability in biological invasions. We constructed a set of integrodifference population models that incorporate classic population fluctuation mechanisms to determine how density dependence in demography, including Allee effects, and in dispersal affects the speed of biological invasions. We show that density dependence is a key factor in producing fluctuations in spreading speed when Allee effects are acting on population densities that fluctuate locally. We show that the necessary density fluctuations can arise from either a nonmonotone population growth function where densities fluctuate locally (e.g., overcompensatory population growth), or from density-dependent dispersal when the population growth function results in constant local densities. As density dependence in both demography and dispersal are common, this mechanism of variability may influence many invading organisms.

Significance Statement

Controlling the spread of biological invasions reduces the cost of mitigating invasive species. However, predicting empirical invasive population spread is difficult as evi-

dence shows the speed of this movement can be highly variable. Here, we provide a novel mechanism for this variability, showing that internal population dynamics can lead to fluctuations in the speed of biological invasions through the combined action of density dependence in demography and dispersal. Speed fluctuations occur through the creation of a variable pushed invasion wave, that moves forward not from small populations at the invasion front, but instead from larger, more established populations that "jump" forward past the previous invasion edge. Variability in the strength of the push generates fluctuating invasion speeds.

Introduction

Fluctuations in population size have fueled a now-classic debate over whether populations are governed by extrinsic environmental factors or by intrinsic self-limitation (reviewed in Kingsland 1995). One of the most important advances of twentieth-century ecology was the discovery that intrinsic density feedbacks can cause population densities to fluctuate, even in constant environments (May, 1974; Turchin, 2003; Costantino et al., 1997). This discovery helped resolve the important role of density dependence in population regulation, revealing that strong regulating forces can generate dynamics that are superficially consistent with no regulation at all. The long history and textbook status of fluctuations in local population size contrast strongly with relatively poor understanding of fluctuations in the spatial dimension of population growth: spread across landscapes.

Understanding and predicting the dynamics of population spread take on urgency in the era of human-mediated biological invasions and range shifts in response to climate change. The velocity of spread, or "invasion speed", is a key summary statistic of an expanding population and an important tool for ecological forecasting (Fagan et al., 2002). Estimates of invasion speed are often derived from regression methods that describe change in spatial extent with respect to time (Miller and Tenhumberg,

2010; Lubina and Levin, 1988; Andow et al., 1990; van den Bosch et al., 1992). Implicit in this approach is the assumption that the true spreading speed is constant and deviations from it represent "error" in the underlying process, or in human observation of the process. This assumption is reinforced by long-standing theoretical predictions that, under a wide range of conditions, a spreading population will asymptotically reach a constant velocity that is determined by the "pulling" force of rare long-distance movement and rapid population growth at the low-density leading edge (Weinberger, 1982; Skellam, 1951; Kot et al., 1996; Neubert and Caswell, 2000). This conventional wisdom of long-term constant invasion speeds is still widely applied, and support for this result is found in lab experiments under controlled conditions (Gandhi et al., 2016).

In contrast to classic theoretical and empirical approaches that emphasize a long-term constant speed, there is growing recognition that spread dynamics can be highly variable and idiosyncratic (Melbourne and Hastings, 2009; Miller and Inouye, 2013; Johnson et al., 2006; Peltonen et al., 2002; Walter et al., 2015; Robertson et al., 2009; Michaels, 1984; Chen, 2014). Some models predict fluctuating spreading speeds due to extrinsic factors such as environmental heterogeneity (Neubert and Caswell, 2000) or interactions with other species (Dwyer and Morris, 2006). Indeed, empirical studies of invasive organisms often attribute temporal variation in speed to differences in the environments encountered by the invading population (e.g., Andow et al. 1990; Peltonen et al. 2002). An alternative hypothesis is that endogenous mechanisms generate fluctuations in spreading speed, even in a homogeneous landscape, mirroring the potential for endogenous fluctuations in local population size in temporally constant environments. Endogenous fluctuations in spreading speed (which we define here as any variability in spreading speed through time, ranging from two-cycle oscillations to chaos), have been surprisingly neglected by the large theoretical literature on biological invasion (but see Johnson et al. 2006, Shaw et al. unpublished) and would

be easily missed by empirical studies that were not looking for them. Understanding whether such fluctuations are possible and the conditions under which they occur would help resolve sources of variability in invasion speed, and facilitate management objectives for range expansion by native and exotic species.

Here, we develop mathematical models of spatial spread to ask whether the velocity of an expanding population can fluctuate, even in a spatially and temporally uniform environment, and to identify conditions under which such endogenous fluctuations may occur. As a starting point, we take inspiration from the relatively complete understanding of endogenous fluctuations in local population density, which arise from time-lagged density feedbacks (i.e., populations persistently overshoot and undershoot their carrying capacity). We conjectured that density feedbacks should be similarly important for fluctuating invasion speeds. Because spread dynamics are jointly governed by demography (local births and deaths) and dispersal (spatial redistribution), we considered several types of density feedbacks (Sakai et al., 2001), including density-dependent movement (Matthysen, 2005) and positive density dependence in population growth (i.e., Allee effects) at the low-density invasion front (Taylor and Hastings, 2005). Allee effects cause invasion waves to be "pushed" from behind their leading edge (Kot et al., 1996; Wang et al., 2002) and we show them to be an important ingredient of fluctuations in the speed of spatial spread.

We began by asking whether conditions that promote fluctuations in local density also promote fluctuations in spatial spread. We then asked whether fluctuations in invasion speed are possible even when population growth produces constant local population densities. We discovered several mechanisms, all arising from density dependence in demography and/or dispersal, that can induce endogenous fluctuations in invasion speed, ranging from stable two-point cycles to apparent chaos. By demonstrating that simple invasion models can generate complex spread dynamics, our results reveal previously undescribed sources of variability in biological invasions

and provide a roadmap for empirical studies to detect these processes in nature.

The Models

We start with an integrodifference population model for population spread through a spatially uniform environment (Kot et al., 1996):

$$n_{t+1}(x) = \int_{-\infty}^{\infty} k(x-y,\sigma^2) f\big(n_t(y)\big)\ dy. \tag{1}$$

Here $n_t(x)$ is the population density at time t and location x, and is a function of two sequential processes: local demography and dispersal. We assume non-overlapping generations where adults $n_t(x)$ generate $f(n_t(x))$ offspring, that then disperse. The distribution of dispersal distances (the dispersal kernel) is given by $k(x-y,\sigma^2)$ and is the probability that an individual disperses from location y to location x (where the probability depends only on the distance $x-y$), with σ^2 as the variance of the kernel. For all models, we describe dispersal using a Laplace probability density function (Wang et al., 2002).

Fluctuating Non-spatial Density

We first ask if a growth function $f(n)$ that promotes fluctuations in local density also promotes fluctuations in spreading speed. We therefore consider the case of over-compensatory population growth, where density can overshoot the carrying capacity. Long-standing theory suggests that compensatory population growth, with or without Allee effects, leads to constant invasion speeds (Weinberger, 1982; Lui, 1985; Wang et al., 2002). Additionally, when Allee effects are not present, overcompensatory growth does not give rise to fluctuations in invasion speed (Li et al., 2009). Here, we investigate whether adding an Allee effect to an overcompensatory growth function can induce fluctuating invasion speeds. We define the growth term of equation 1 as the Ricker function

$$f\big(n\big) = \begin{cases} n\exp\Big(r(1-n)\Big) & \text{for } n > n_{thresh} \\ 0 & \text{for } n \leq n_{thresh} \end{cases} \tag{2}$$

which is modified to include the possibility of a strong Allee effects (Fig S1a). Here, r is the intrinsic growth rate, and n_{thresh} is the Allee effect threshold, which is the critical density below which the population goes extinct. We refer to this model as the "overcompensatory model" throughout.

We simulated the model across a range of r and n_{thresh} parameter values (Fig. 1a), each for 200 iterations using MATLAB (MATLAB, 2014). Here, we fixed the variance of the dispersal kernel to $\sigma^2 = 0.25$. Within each simulation, we defined the invasion front at each time step as the location where the density of the invasion wave was first above the detection threshold of 0.05 (Fig. 2a-e). We then used this location to calculate the instantaneous invasion speed as the distance travelled by the front between consecutive time steps (Fig. 2f). To determine if the invasion speed fluctuated, we quantified how this speed changed through time.

Overcompensatory Model Results

We found that the overcompensatory model can generate fluctuating invasion speeds, but only if Allee effects and fluctuations in local population density are present (Fig. 1a, S2). In populations experiencing Allee effects, the fluctuations in local population density are propagated in space, which promotes fluctuations in invasion speed. This can occur even when the local population would crash in a nonspatial model due to high population density fluctuations. Fluctuations in speed occur within limited parameter space; when the Allee effect threshold (n_{thresh}) is too large the spreading population crashes, and if the growth rate (r) is too small the population invades at a constant speed (Fig. 1a). The observed fluctuations have a small amplitude, and range from 2-cycle oscillations to apparently chaotic (Fig. S3).

In this model, fluctuations in speed are induced via a pushed invasion wave, and the Allee threshold determines the magnitude of fluctuations by altering the size of the push. The invasion front moves forward, not from the low density leading edge, but instead from populations farther back in the wave that jump forward past the invasion front and *push* the wave ahead. When the population density at any location is smaller than the Allee threshold, which occurs at the edge of the wave, the population decays to zero before the next time step. Populations just above the Allee threshold become large after reproduction, but as the adult population size of $n(x)$ increases beyond the Allee threshold, the offspring population size $f(n(x))$ declines, as defined by the Ricker growth function (Fig. S1a). Therefore, when reproduction occurs (transition between $n(x)$ and $f(n(x))$, Fig. 2a-b), the populations with highest density become populations of low density, and populations with density just above the Allee threshold become high density. Through time, this creates variability in the size of the push, or the region contributing to the wave front (Fig. 2b vs d), which leads to fluctuations in the invasion speed.

Constant Non-spatial Density

We next examine a model where the population growth function ($f(n)$) results in constant local population densities to determine if this case can also produce fluctuating invasion speeds. Here, we consider a version of the basic model (eqn. 1) where the growth function is piecewise linear, with the form

$$f(n) = \begin{cases} \lambda n & \text{for } n < n_{thresh} \\ n_k & \text{for } n \geq n_{thresh} \end{cases} \tag{3}$$

where n_k is the carrying capacity density, and n_{thresh} is the critical density above which the population reaches its max density (Fig. S1b). As before, n_{thresh} is the Allee effect threshold; below this point population growth is less than one when strong Allee effects are present. However, we now include a parameter λ that describes the

strength of the Allee effect. For $\lambda = n_k/n_{thresh}$ there is no Allee effect. For $0 \leq \lambda \leq 1$ there is a strong Allee effect where population size decreases at low density (Fig. S1b). For $1 < \lambda < n_k/n_{thresh}$ there are weak Allee effects, but we only briefly touch on these results, as they do not produce fluctuations in speed.

Here we explore density dependence in two aspects of dispersal: the propensity (the fraction of individuals that disperse), and the distances that dispersing individuals travel. We again use the general integrodifference form for our invasion model (eqn. 1), but incorporate a piecewise linear growth function (eqn. 3).

When dispersal *propensity* is density-dependent we let the probability of dispersal be given by

$$p\big(\xi_t(x)\big) = p_0 + \left[\frac{1}{1 + e^{-\alpha\left(\xi_t(x) - \hat{\xi}\right)}}\right](p_{max} - p_0) \tag{4}$$

which is a logistic form similar to other models with density-dependent dispersal (Smith et al., 2008). Here, $\xi_t(x) = \epsilon n_t(x) + (1-\epsilon) f(n_t(x))$ is a weighted combination of the local density of adults $n_t(x)$, and offspring $f(n_t(x))$, where ϵ is the relative weighting of these two densities. The dispersal propensity can depend on only the adult population density ($\epsilon = 1$), on only the offspring density ($\epsilon = 0$), or on some combination of both ($0 < \epsilon < 1$). In this formulation, $\hat{\xi}$ is the dispersal threshold, α is a shape parameter that controls the steepness at the threshold, and p_0 and p_{max} are lower and upper bounds on the propensity, respectively (Fig. S1c). The sign of α determines if dispersal increases or decreases with density, indicating positive or negative density dependence, respectively. From this, we get the integrodifference model

$$n_{t+1}(x) = \Big[1 - p\big(\xi_t(x)\big)\Big] f\big(n_t(x)\big) + \int_{-\infty}^{\infty} p\big(\xi_t(y)\big) k(x-y, \sigma^2) f\big(n_t(y)\big)\, dy \tag{5}$$

which we refer to as the "propensity model" throughout.

Alternatively, when the dispersal *distance* is density-dependent, we let the disper-

sal kernel variance be modified by the weighted population density (ϵ) and have the form

$$\sigma^2\big(\xi_t(x)\big) = \sigma_0^2 + \left[\frac{1}{1+e^{-\beta\left(\xi_t(x)-\hat{\xi}\right)}}\right](\sigma_{max}^2 - \sigma_0^2) \tag{6}$$

where β is a shape parameter that controls the steepness at the threshold, and σ_0^2 and σ_{max}^2 are lower and upper bounds on the variance, respectively (Fig. S1d). Here, the sign of β determines if density dependence is positive or negative. This results in our final integrodiffernce model

$$n_{t+1}(x) = \int_{-\infty}^{\infty} k\Big(x-y, \sigma^2\big(\xi_t(y)\big)\Big) f\big(n_t(y)\big)\ dy \tag{7}$$

which we refer to as the "distance model" throughout.

We simulated both of these models (eqns. 5 and 7) for 200 iterations, across parameter values $\epsilon = [0, 0.5, 1]$, $0 \leq \lambda \leq 2$ (strong to weak Allee effects), and $\lambda = 5$ (no Allee effect), $0 \leq \hat{\xi} \leq 1$, and $n_{thresh} = 0.2$ for both models, with $-100 \leq \alpha \leq 100$, $p_0 = 0.05$, and $p_{max} = 1$ for the propensity model, and $-100 \leq \beta \leq 100$, $\sigma_0^2 = 0.05$, and $\sigma_{max}^2 = 1$ for the distance model. As before, we calculated the instantaneous invasion speed to determine if it fluctuated through time.

Propensity Model Results

With the propensity model (eqn. 5), speed fluctuations occur only when the propensity to disperse depends at least in part on the adult population density ($\epsilon > 0$), Allee effects are present ($0 \leq \lambda < 1$), and dispersal propensity increases with increasing population density ($\alpha > 0$). We did not find evidence of fluctuations with weak Allee effects ($1 < \lambda < n_k/n_{thresh}$) (Fig. S4a). The amplitude of these fluctuations increase as the strength of the Allee effect, and density dependence increases (Fig. 1b). Fluctuations in this model always occur as 2-cycle oscillations, and are stronger when it takes a larger density to trigger movement (increasing $\hat{\xi}$) (Fig. S4a). Alternatively,

when dispersal propensity decreases with increasing denisty ($\alpha < 0$), the invasion moves at a constant speed.

Here, density-dependent dispersal induces the density fluctuations needed to create speed fluctuations, but only when combined with Allee effects, which generates a pushed wave (SI Appendix). As before, spreading speed fluctuations are created through variations in the magnitude of the push that reaches the edge of the invasion. The magnitude of a push depends on the width of the region contributing to the push, and the proximity of this region in relation to the wave front (Fig. 2g-k). Directly adjacent to the wave edge the population is below the Allee effect threshold (n_{thresh}) and therefore decays to zero (Fig. 2g). Farther from the edge, the population density is above the Allee effect threshold, but below the dispersal threshold ($\hat{\xi}$). Thus this region of the population behind the wave front reproduces, but does not disperse (Fig. 2h,i). This results in a large push from behind the wave front that moves the invasion front forward at the next time step (Fig. 2i-k). Subsequently, the region of the non-dispersing population is much smaller and farther from the invasion front at the next time step, resulting in a much smaller push (Fig. 2k).

Distance Model Results

For the distance model (eqn. 7), we again find that invasion speed only fluctuates via pushed waves when density-dependent dispersal depends at least partially on the adult population density ($\epsilon > 0$), and strong Allee effects are present ($0 \leq \lambda \leq 1$). However, unlike the propensity model, we find fluctuations when density-dependent dispersal is both positive ($\beta > 0$) and negative ($\beta < 0$) (Fig. 1c, S4b, SI Appendix). The speed fluctuations exhibit more chaotic dynamics (Fig. S5) than the two-cycle fluctuations seen in the propensity model, with larger amplitude fluctuations when the dispersal distance increases with density ($\beta > 0$), than when it decreases with density ($\beta < 0$) (Fig. 1c, S5). In general, fluctuations are larger as both Allee effects and density dependence are stronger. Additionally, when increasing densities increase

the dispersal distance ($\beta > 0$), the fluctuation amplitude increases as it takes a larger density to trigger long distance movement, and this trend is opposite when increasing densities decrease dispersal distance ($\beta < 0$) (Fig. S4b).

When the dispersal distance shows positive density dependence (Fig. 2m-r), populations at densities above the dispersal threshold will disperse long distances, and those below will disperse short distances. While the short distance dispersers are always directly adjacent to the wave edge after reproduction, each push forward is made up of a combination of both short and long distance dispersers. The size of this push changes depending on the proportion of the push made up of each type of disperser, and this proportion changes with time, creating fluctuating invasion speeds. For example, when a small peak in population density is above the dispersal threshold, a small population mass disperses long distances and the front advances a short distance (Fig. 2m-o). However, when a larger peak of the population density is above the dispersal threshold, a larger population disperses long distances, and the wave advances a longer distance (Fig. 2o-q).

We also find spreading speed fluctuations when the dispersal distance has negative density dependence, that also result from variation in the proportion of the population that disperse short and long distances. Here, however, when populations are above the dispersal threshold, they disperse a short distance, and when they are below the dispersal threshold, they disperse long distances. In the negative density-dependent dispersal case, long distance disperses are always adjacent to the wave edge, and pushes with a small proportion of long distance dispersers move less far (Fig. 2s-u) than those made up of more long distance dispersers (Fig. 2u-w).

Discussion

Here we demonstrate that fluctuations in invasion speed can be induced solely through endogenous population dynamics, a previously undescribed mechanism behind inva-

sion variability. Specifically, we show that Allee effects acting on fluctuating local population densities are necessary to create these variable invasion speeds. This occurs when the population growth function produces both fluctuating and constant local population densities. In the former case, overcompensatory growth produces the necessary fluctuating local population densities, in the latter case these density fluctuations are created through density-dependent dispersal. In our models, fluctuations in spreading speed occur through a form of variable pushed wave. While pushed waves are common (Gandhi et al., 2016; Mendez et al., 2011; van Saarloos, 2003; Garnier et al., 2012), especially given the known influence of Allee effects at the low density wave edge (Taylor and Hastings, 2005; Shigesada and Kawasaki, 1997), our models show that this pushing force generated by the Allee effect can lead to endogenous variability in spreading speed when accompanied by mechanisms that create density-dependence, as this combined action creates variability in the pushing force through time. This result has potential to be more consistent with the highly variable data seen from empirical invasion studies (Johnson et al., 2006; Peltonen et al., 2002; Walter et al., 2015; Robertson et al., 2009; Michaels, 1984; Chen, 2014)

Allee effects are often considered in relation to invasions (Taylor and Hastings, 2005), as the leading edge of an invasion tends to experience low population densities (Shigesada and Kawasaki, 1997), and Allee effects are seen in many organisms (Kramer et al., 2009; Morris, 2002). In isolation Allee effects have been shown to influence small populations at the invasion edge by decreasing low-density vital rates (e.g., reproduction Veit and Lewis 1996), which can lead to decreased invasion speeds (Wang and Kot, 2001). We show here that Allee effects can also generate fluctuations in spreading speed, but they must be acting on populations that also have some form of local density fluctuations. This combination of Allee effects and density fluctuations due to dispersal have been shown to induce oscillations in a serious North American forest invader, the Gypsy Moth (Johnson et al., 2006). In our models, these

fluctuations are driven by variable pushed waves. One major new insight our results provide, is that vital rates must be not only examined in populations at low density, but also in those at high-density, as the invasion front is being driven by high-density populations.

In our models, density-dependent dispersal, which is displayed in many organisms (Bonenfant et al., 2009; Matthysen, 2005; Fronhofer et al., 2015; Denno and Peterson, 1995), was a main source of local population density fluctuations. Its effect ranged depending on whether responses to density were positive or negative, and if it altered either the propensity to disperse or the dispersal distance. In the propensity model, fluctuations were seen when the propensity to disperse increased with increasing density. Positive density-dependent dispersal propensity is most notable in insects, as wingless aphids can produce winged morphs when densities become high (Harrison, 1980; Johnson, 1965), and some butterflies increase movement in response to mate density avoidance (Baguette et al., 1998). This movement can create an Allee effect if it reduces mate finding abilities at low densities, especially when the movement is sex biased (Shaw et al. unpublished). In the distance model, fluctuations were seen under both positive and negative density dependence. Mobile organisms can increase their dispersal distance with increasing density by altering behavioral responses (Matthysen, 2005). Alternatively, dispersal distances can decrease with density when crowding decreases reproductive output and dispersal ability (Marchetto et al., 2010; Donohue, 1998; Matthysen, 2005), or in animals (notably small mammals) with strong group behavior (Ims and Andreassen, 2005; Andreassen and Ims, 2001; Matthysen, 2005). The empirical studies on density-dependent dispersal tend to match where we find fluctuating invasion speeds in our models, indicating we have explored relevant parameter space.

Coupling models and empirical data has proven to be a fruitful approach to understanding the mechanisms behind fluctuations in non-spatial population density

(e.g., Turchin 2003; Costantino et al. 1997), yet we have much less coupled data in spatial systems (Bolker et al., 2003). We propose that examining highly variable empirical invasion data (Melbourne and Hastings, 2009) in light of our theoretical results could provide a novel mechanism by which variable invasions occur. To identify the density-dependent mechanisms acting on invaders, empirical data on the combination of fluctuation periodicity, amplitude, and the long-term shape of the wave would be necessary. Given the difficulty of collecting long-term data, some patterns might be easier to identify than others. The strong 2-cycle speed fluctuations generated when invaders experience both Allee effects and density-dependent dispersal propensity would likely be the most evident in data. We recognize that while many invaders may experience Allee effects, or density-dependent dispersal, the likelihood of both endogenous processes acting on an invading population simultaneously (which is required to generate speed fluctuations) is unknown. Teasing out the signature of these endogenous mechanisms from data may prove difficult, given an inherently heterogeneous and stochastic world, yet we encourage empiricists to re-examine variable invasion data in the context of these density-dependent mechanisms.

Understanding the basic mechanisms behind invasion variability would allow for better forecasting, and ultimately improved control, of biological invasions. While fluctuations in invasion speed have been found due to exogenous factors including habitat patchiness, predator-prey dynamics, and climatic variability (Dwyer and Morris, 2006; Neubert et al., 2000; Peltonen et al., 2002), we show here, that internal density-dependent population dynamics can also induce fluctuating invasion speeds. These results provide a new focus for understanding variable invasions.

Acknowledgements

LLS and AKS were supported by startup funds from the University of Minnesota to AKS, BTL was supported by NSF DMS-1515875. The initial idea was developed

during the 2014 ACKME Nantucket Mathematical Ecology retreat with input from participants and funding from Sea Grant. The manuscript was greatly improved by comments from E. Strombom and R. Williams. The authors acknowledge the Minnesota Supercomputing Institute (MSI) at the University of Minnesota for providing resources that contributed to the research results reported within this paper. URL: http://www.msi.umn.edu.

References

Andow, D. A., Kareiva, P. M., Levin, S. A., and Okubo, A. (1990). Spread of invading organisms. *Landscape Ecology*, 4(2-3):177–188.

Andreassen, H. P. and Ims, R. A. (2001). Dispersal in patchy vole populations: Role of patch configuration, density dependence, and demography. *Ecology*, 82(10):2911–2926.

Baguette, M., Vansteenwegen, C., Convi, I., and Nève, G. (1998). Sex-biased density-dependent migration in a metapopulation of the butterfly Proclossiana eunomia. *Acta Oecologica*, 19(1):17–24.

Bolker, B. M., Pacala, S. W., and Neuhauser, C. (2003). Spatial dynamics in model plant communities: what do we really know? *The American Naturalist*, 162(2):135–48.

Bonenfant, C., Gaillard, J. M., Coulson, T., Festa-Bianchet, M., Loison, A., Garel, M., Loe, L. E., Blanchard, P., Pettorelli, N., Owen-Smith, N., Du Toit, J., and Duncan, P. (2009). Empirical evidence of density-dependence in populations of large herbivores. *Advances in Ecological Research*, 41:313–357.

Chen, H. (2014). A spatiotemporal pattern analysis of historical mountain pine beetle outbreaks in British Columbia, Canada. *Ecography*, 37(4):344–356.

Costantino, R. F., Desharnais, R. A., Cushing, J. M., and Dennis, B. (1997). Chaotic dynamics in an insect population. *Science*, 275(5298):389–391.

Denno, R. F. and Peterson, M. A. (1995). Density-dependent dispersal and its consequences for population dynamics. In Cappuccino, N. and Price, P. W., editors, *Population Dynamics: New Approaches and Synthesis*, pages 113–130. Academic Press.

Donohue, K. (1998). Maternal determinants of seed dispersal in Cakile edentula: Fruit, plant, and site traits. *Ecology*, 79(8):2771–2788.

Dwyer, G. and Morris, W. F. (2006). Resource-dependent dispersal and the speed of biological invasions. *The American Naturalist*, 167(2):165–76.

Fagan, W. F., Lewis, M. A., Neubert, M. G., and van den Driessche, P. (2002). Invasion theory and biological control. *Ecology Letters*, 5(1):148–157.

Fronhofer, E. A., Kropf, T., and Altermatt, F. (2015). Density-dependent movement and the consequences of the Allee effect in the model organism Tetrahymena. *Journal of Animal Ecology*, 84:712–722.

Gandhi, S. R., Yurtsev, E. A., Korolev, K. S., and Gore, J. (2016). Range expansions transition from pulled to pushed waves as growth becomes more cooperative in an experimental microbial population. *Proceedings of the National Academy of Sciences*, 113(25):6922–6927.

Garnier, J., Giletti, T., Hamel, F., and Roques, L. (2012). Inside dynamics of pulled and pushed fronts. *Journal des Mathematiques Pures et Appliquees*, 98:428–449.

Harrison, R. G. (1980). Dispersal polymorphisms in insects. *Annual Review of Ecology and Systematics*, 11:95–118.

Ims, R. A. and Andreassen, H. P. (2005). Density-dependent dispersal and spatial population dynamics. *Proceedings of the Royal Society B*, 272(1566):913–918.

Johnson, B. (1965). Wing polymorphism in aphids II. Interactions between aphids. *Entomologia Experimentalis et Applicata*, 8(1):49–64.

Johnson, D. M., Liebhold, A. M., Tobin, P. C., and Bjørnstad, O. N. (2006). Allee effects and pulsed invasion by the gypsy moth. *Nature*, 444(7117):361–363.

Kingsland, S. E. (1995). *Modeling nature*. University of Chicago Press.

Kot, M., Lewis, M. A., and van den Driessche, P. (1996). Dispersal data and the spread of invading organisms. *Ecology*, 77(7):2027–2042.

Kramer, A. M., Dennis, B., Liebhold, A. M., and Drake, J. M. (2009). The evidence for Allee effects. *Population Ecology*, 51(3):341–354.

Li, B., Lewis, M. A., and Weinberger, H. F. (2009). Existence of traveling waves for integral recursions with nonmonotone growth functions. *Journal of Mathematical Biology*, 58(3):323–338.

Lubina, J. A. and Levin, S. A. (1988). The spread of a reinvading species: Range expansion in the California Sea Otter. *The American Naturalist*, 131(4):526–543.

Lui, R. (1985). A nonlinear integral operator arising from a model in popualtion genetics III. Heterozygote inferior case. *SIAM Journal of Mathematical Analysis*, 16(6):1180–1206.

Marchetto, K. M., Jongejans, E., Shea, K., and Isard, S. A. (2010). Plant spatial arrangement affects projected invasion speeds of two invasive thistles. *Oikos*, 119(9):1462–1468.

MATLAB (2014). MATLAB and Statsistics Toolbox Release. Technical report, The MathWorks, Inc., Nantick, Massachusetts, United States.

Matthysen, E. (2005). Density-dependent dipsersal in birds and mammals. *Ecography*, 28(3):403–416.

May, R. M. (1974). Biological populations with nonoverlapping generations: Stable points, stable cycles, and chaos. *Science*, 186(4164):645–647.

Melbourne, B. A. and Hastings, A. (2009). Highly variable spread rates in replicated biological invasions: Fundamental limits to predictability. *Science*, 325:1536–1539.

448 Mendez, V., Llopis, I., Campos, D., and Horsthemke, W. (2011). Effect of environ-
449 mental fluctuations on invasion fronts. *Journal of Theoretical Biology*, 281(1):31–38.

450 Michaels, P. J. (1984). Climate and the southern pine beetle in Atlantic coastal and
451 Piedmont regions. *Forest Science*, 30(1):143–156.

452 Miller, T. E. X. and Inouye, B. D. (2013). Sex and stochasticity affect range expansion
453 of experimental invasions. *Ecology Letters*, 16:354–361.

454 Miller, T. E. X. and Tenhumberg, B. (2010). Contributions of demography and
455 dispersal parameters to the spatial spread of a stage-structured insect invasion.
456 *Ecological Applications*, 20(3):620–633.

457 Morris, D. W. (2002). Measuring the Allee effect: Positive density dependence in
458 small mammals. *Ecology*, 83(1):14–20.

459 Neubert, M. G. and Caswell, H. (2000). Demography and dispersal: Calculation
460 and sensitivity analysis of invasion speed for structured populations. *Ecology*,
461 81(6):1613–1628.

462 Neubert, M. G., Kot, M., and Lewis, M. A. (2000). Invasion speeds in fluctuating
463 environments. *Proceedings of the Royal Society of London*, 267:1603–1610.

464 Peltonen, M., Liebhold, A. M., Bjørnstad, O. N., and Williams, D. W. (2002). Spatial
465 synchrony in forest insect outbreaks: Roles of regional stochasticity and dispersal.
466 *Ecology*, 83(11):3120–3129.

467 Robertson, C., Nelson, T. A., Jelinski, D. E., Wulder, M. A., and Boots, B. (2009).
468 Spatial-temporal analysis of species range expansion: The case of the mountain
469 pine beetle, Dendroctonus ponderosae. *Journal of Biogeography*, 36(8):1446–1458.

470 Sakai, A. K., Allendorf, F. W., Holt, J. S., Lodge, D. M., Molofsky, J., With, K. A.,
471 Baughman, S., Cabin, R. J., Cohen, J. E., Ellstrand, N. C., McCauley, D. E.,

O'Neil, P., Parker, I. M., Thompson, J. N., and Weller, S. G. (2001). The population biology of invasive specie. *Annual Review of Ecology and Systematics*, 32:305–332.

Shigesada, N. and Kawasaki, K. (1997). *Biological invasions: Theory and practice*. Oxford University Press, UK.

Skellam, J. G. (1951). Random dispersal in theoretical populations. *Biometrika*, 38(1):196–218.

Smith, M. J., Sherratt, J. A., and Lambin, X. (2008). The effects of density-dependent dispersal on the spatiotemporal dynamics of cyclic populations. *Journal of Theoretical Biology*, 254(2):264–274.

Taylor, C. M. and Hastings, A. (2005). Allee effects in biological invasions. *Ecology Letters*, 8:895–908.

Turchin, P. (2003). *Complex population dynamics: A theoretical/empirical synthesis*. Princeton University Press.

van den Bosch, F., Hengeveld, R., and Metz, J. A. J. (1992). Analysing the velocity of animal range expansion. *Journal of Biogeography*, 19(2):135–150.

van Saarloos, W. (2003). Front propagation into unstable states. *Physics Reports*, 386:29–222.

Veit, R. R. and Lewis, M. A. (1996). Dispersal, population growth, and the Allee Effect: Dynamics of the house finch invasion of eastern North America. *The American Naturalist*, 148(2):255–274.

Walter, J. A., Johnson, D. M., Tobin, P. C., and Haynes, K. J. (2015). Population cycles produce periodic range boundary pulses. *Ecography*, 38:1200–1211.

Wang, M.-H. and Kot, M. (2001). Speeds of invasion in a model with strong or weak Allee effects. *Mathematical Biosciences*, 171(1):83–97.

Wang, M.-H., Kot, M., and Neubert, M. G. (2002). Integrodifference equations, Allee effects, and invasions. *Journal of Mathematical Biology*, 44:150–168.

Weinberger, H. F. (1982). Long-time beahvior of a class of biological models. *SIAM Journal of Mathematical Analysis*, 13(3):353–396.

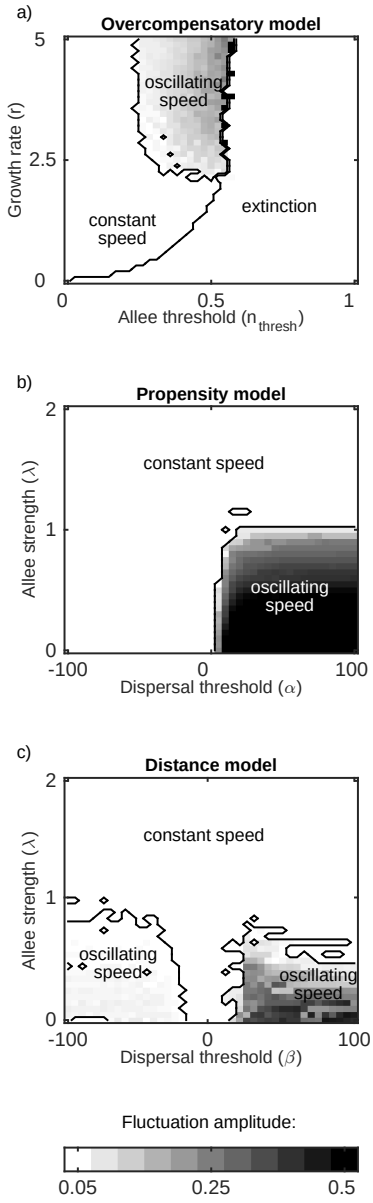

Figure 1: Location and amplitude of fluctuations across parameter space. Parameter values: (a) $\sigma^2 = 0.25$, (b-c) $n_{thresh} = 0.2$, $\lambda = 0$, $\epsilon = 1$, $\hat{\xi} = 0.9$, $n_k = 1$, (b) $\sigma^2 = 0.25$, $p_0 = 0.05$, $p_{max} = 1$, (c) $\sigma_0^2 = 0.05$, $\sigma_{max}^2 = 1$, Initial population density was set to 0, except for a Gaussian distribution over $|x| < 5$ with a peak of 2 and standard deviation of 1. Fluctuations were defined to have an amplitude greater than 0.04 difference in mean speed per time step for all models.

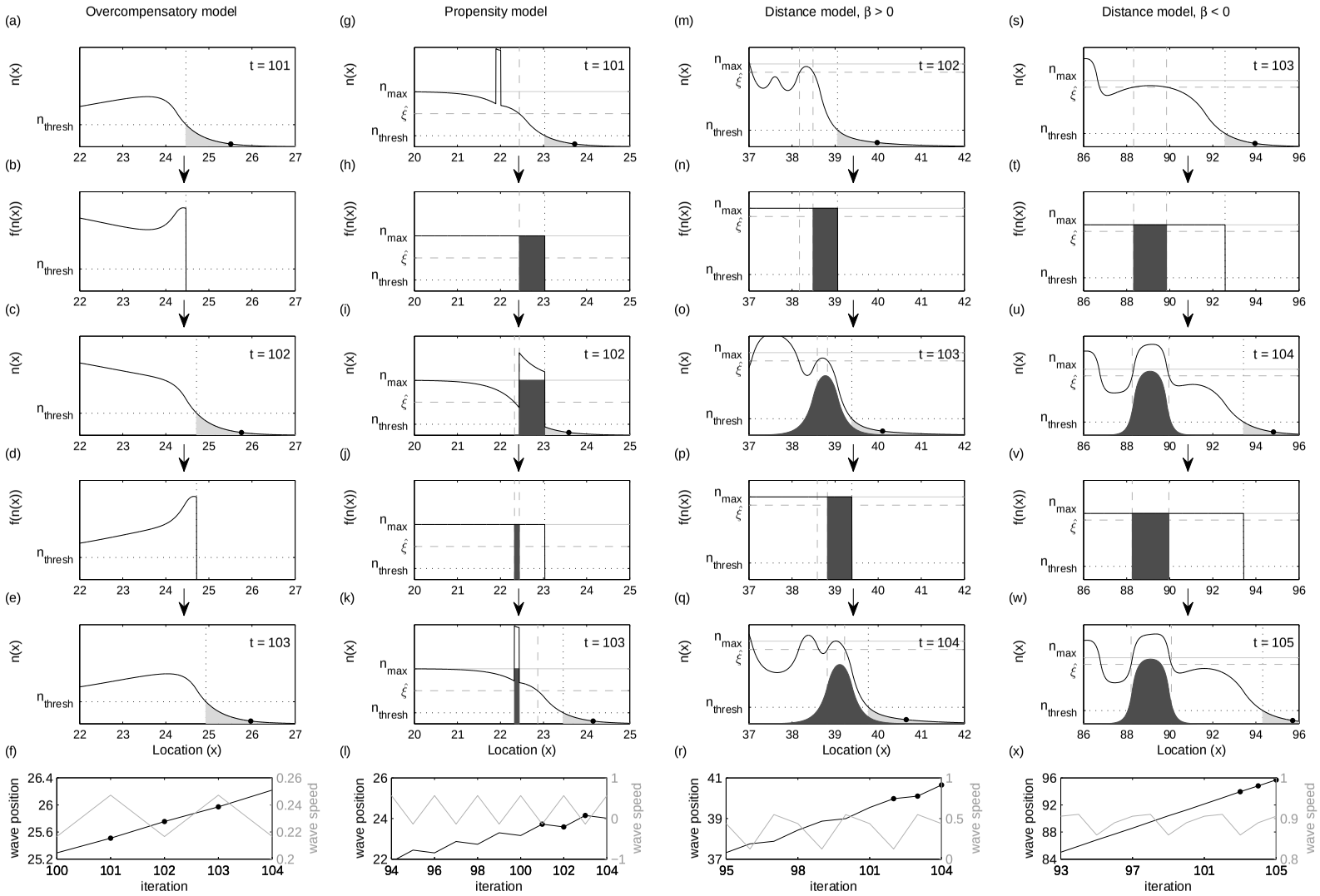

Figure 2: Four examples of fluctuations in invasion speed. The top five rows show the population density before ($n(x)$) and after ($f(n(x))$) growth at sequential time steps, showing individuals that will not reproduce (light gray; $n < n_{thresh}$), those that do not disperse far (dark gray; $n > \hat{\xi}$ or $n < \hat{\xi}$), and the edge of the wave (solid point). The bottom row shows the wave position and speed over time. Parameter values are the same as Fig. 1 except: (a-f) $\sigma^2 = 0.25$, $r = 2.2, n_{thresh} = 0.4$, (g-l) $\sigma^2 = 0.25$, p_0, $\hat{\xi} = 0.6$, $\hat{\xi} = 0.6$, $\alpha \to \infty$, (m-r) $\beta \to \infty$, (s-x) $\beta \to -\infty$. Initial population density was set to 0, except for a Gaussian distribution over $|x| < 5$ with a peak of 2 and standard deviation of 1.

Supporting Information

Table S1: All model parameters, meanings and corresponding equations.

Variable	**Meaning**
t	time
x, y	locations
$n_t(x)$	population density of at location x and time t
Parameter	**Meaning**
σ^2	variance of the dispersal kernel
n_{thresh}	Allee effect threshold
r	intrinsic growth rate (Overcompensatory model)
λ	strength of Allee effect (Propensity and distance models)
ϵ	relative weight of adult versus offspring population density (Propensity and distance models)
$\hat{\xi}$	dispersal threshold (Propensity and distance models)
n_k	carrying capacity density (Propensity and distance models)
p_0	minimum dispersal propensity (Propensity model)
p_{max}	maximum dispersal propensity (Propensity model)
α	dispersal propensity parameter (Propensity model)
σ_0^2	minimum dispersal variance (Distance model)
σ_{max}^2	maximum dispersal variance (Distance model)
β	dispersal propensity parameter (Distance model)
Function	**Meaning**
$k(x-y, \sigma^2)$	dispersal kernel
$f(n_t(x))$	growth / offspring density

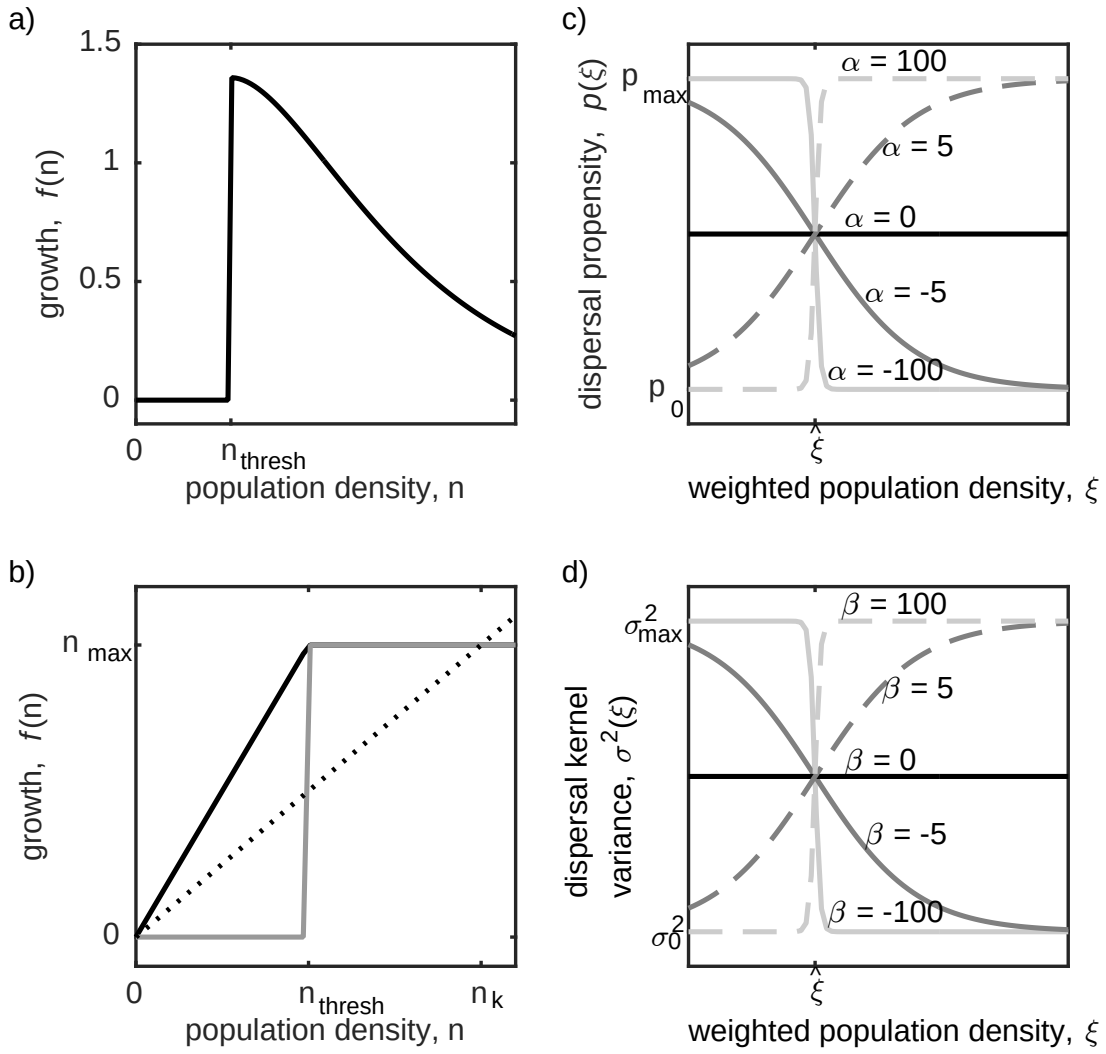

Figure S1: Examples of functions used in simulations (a) growth rate for the Overcompensatory model (eqn. 2) (b) growth rate for Propensity and Distance models (eqn. 3) for $\lambda = n_k/n_{thresh}$ (black) and $\lambda = 0$ (gray), (c) dispersal propensity for density-dependent case (eqn. 4) for different α values, and (d) dispersal kernel variance for density-dependent dispersal distance (eqn. 6) for different β values.

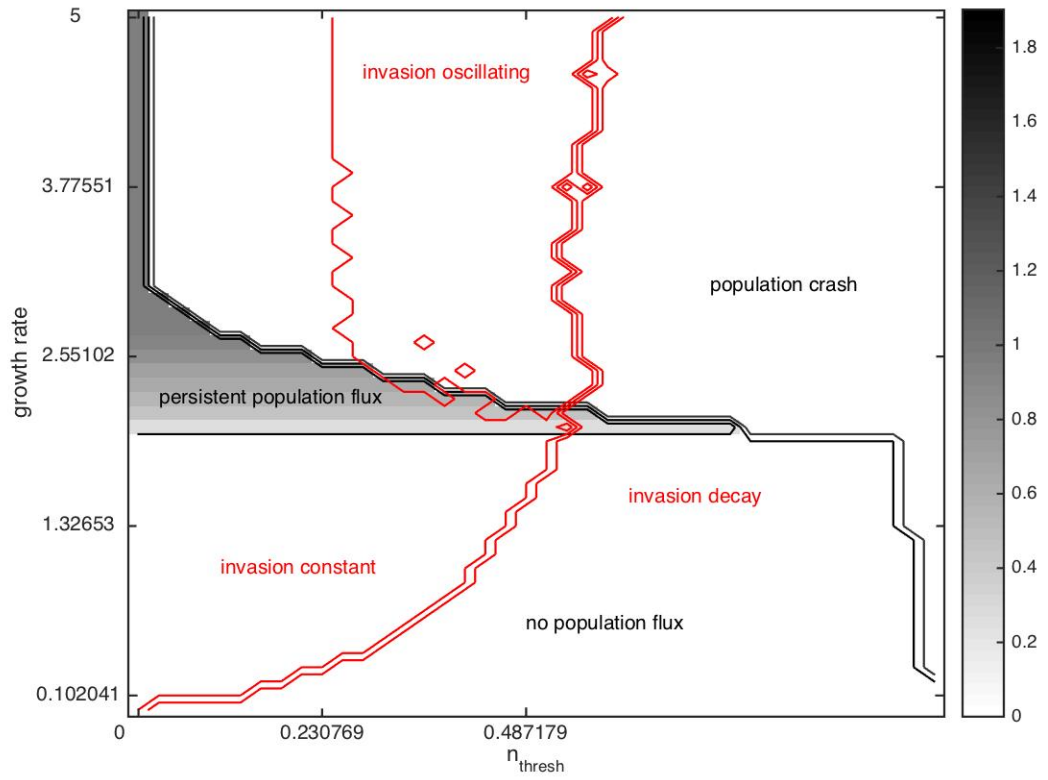

Figure S2: Parameter space over which asymptotic fluctuations in local population density occur (black), overlaid with fluctuations in invasion speed occurrence (red) in the overcompensatory model (eqn. 2). The grayscale indicates the amplitude of density fluctuations. Initial population density was set to 0, except for a Gaussian distribution over $|x| < 5$ with a peak of 2 and standard deviation of 1. All fluctuations were defined to have an amplitude greater than 0.04

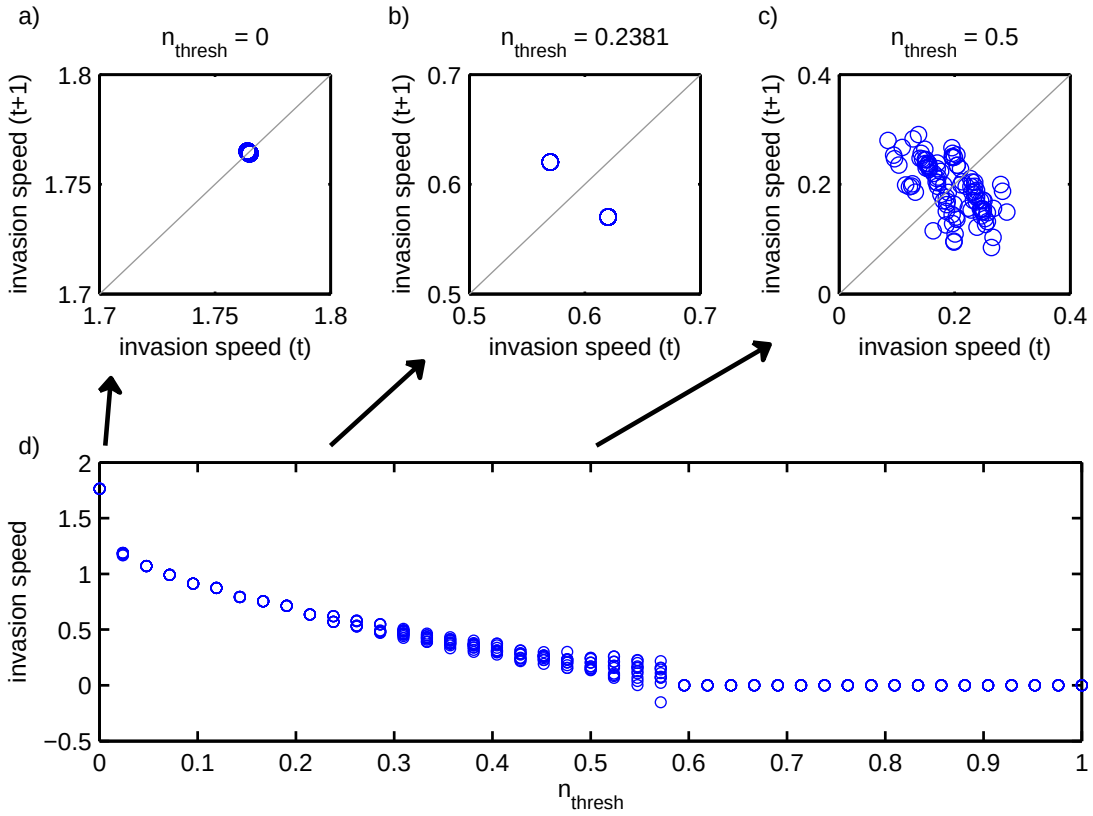

Figure S3: The periodicity of the invasion speed through time for the Overcompensatory model. In panels a-c, the wave position is plotted at time t vs time $t+1$. The wave speed ranges in periodicity across values of the Allee effect threshold n_{thresh}. At small values of n_{thresh} the invasion speed is constant (a), at some moderate values the wave speed is periodic (b), and at larger n_{thresh} values (c), the wave speed becomes chaotic until n_{thresh} becomes so large the population goes extinct. In panel (d), the range of invasion speeds represents the amplitude of fluctuations. At each plotted n_{thresh} value, the invasion speed for the previous 100 time steps are plotted. When points appear as hollow points, the same invasion speed is being plotted over itself many times. Here, $\sigma^2 = 0.25$

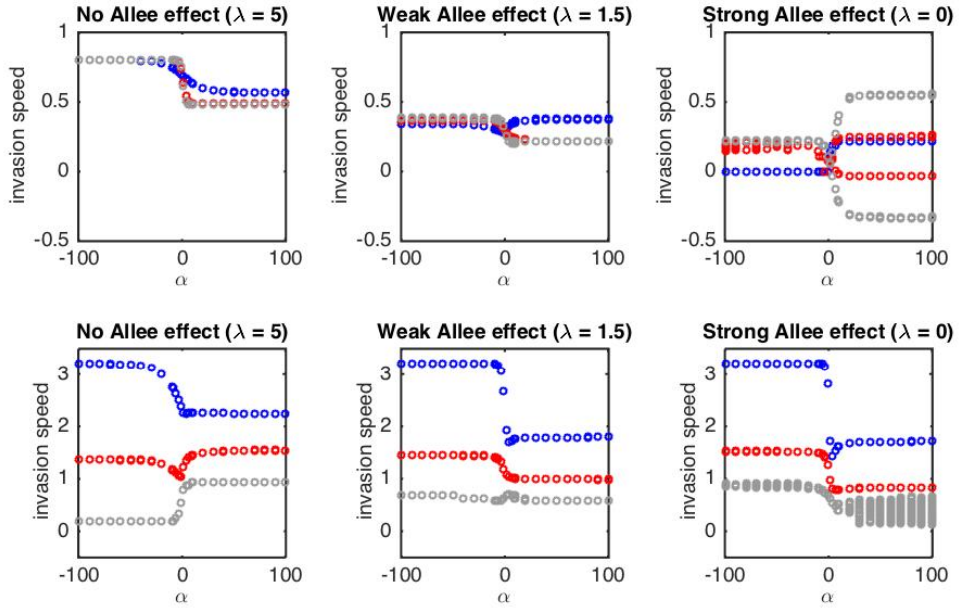

Figure S4: Parameter space exploration for the models used (a) Propensity model - top row (b) Distance model - bottom row Here, blue circles = $\hat{\xi} = 0.1 < n_{thresh}$, red circles = $\hat{\xi} = 0.6 > n_{thresh}$, gray circles = $\hat{\xi} = 0.9 >> n_{thresh}$

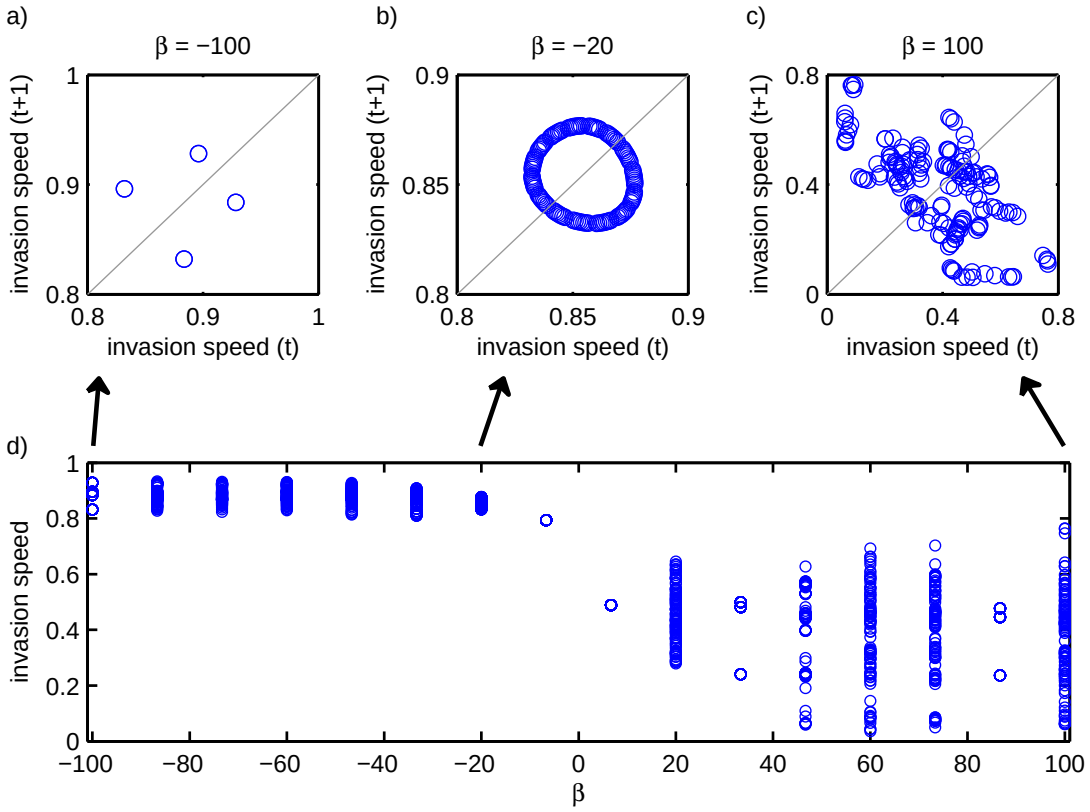

Figure S5: The periodicity of the invasion speed through time for the Distance model. In panels a-c, the wave position is plotted at time t vs time $t+1$. We demonstrate that the invasion speed appears to have an attractor for some values of the density-dependent dispersal threshold (β) (a, b), and is more chaotic for other values of β (c). In panel (d), the range of invasion speeds represents the amplitude of fluctuations for one value of the Allee effect threshold ($\hat{\xi}$). At each plotted β value, the invasion speed for the previous 100 time steps are plotted. When points appear as hollow points, the same invasion speed is being plotted over itself many times. Here, $\hat{\xi} = 0.9$, $\epsilon = 1$, $\lambda = 0$, $\sigma_0^2 = 0.05$, $\sigma_{max}^2 = 1$, and $n_{thresh} = 0.2$.

Appendix: Fluctuations in population density

A. The propensity model.

We demonstrate that the term outside the integral in model (6), which determines the dynamics of the individuals remaining sedentary, can generate fluctuations in population density for positive α and ϵ. This term may be described by $G(n) = [1 - p(\xi(n))]f(n)$ where $p(\xi)$ is given by (4) with $\xi_t(x)$ replaced by ξ, and ξ is given by (5) with $n_t(x)$ replaced by n. ξ is a function of n. Clearly $G(0) = 0$, and

$$G'(n) = -p'(\xi(n))\xi'(n)f(n) + [1 - p(\xi(n))]f'(n).$$

It is easily seen that $p'(\xi) > 0$ for $\alpha > 0$, and $\xi'(n) > 0$ for $0 < \epsilon \leq 1$ and $n \neq n_{thresh}$.

If $\lambda = 0$, $G(n)$ equals zero for $0 \leq n < n_{thresh}$, has a jump at n_{thresh}, and then becomes decreasing since $G'(n) = -p'(\xi)\xi'(n)n_{max} < 0$ for $n > n_{thresh}$.

If $\lambda > 0$, $G'(0) = [1-p(\xi(0))]f'(0) = [1-p(\xi(0))]\lambda > 0$, and $G'(n) = -p'(\xi(n))\xi'(n)n_{max} < 0$ for $n > n_{thresh}$. This shows that $G(n)$ increases initially, and decreases for $n > n_{thresh}$.

We have shown that for positive α and ϵ and for $\lambda \geq 0$, $G(n)$ is a nonmonotone function and it generates fluctuations in population density.

B. The distance model.

We show that the integrand of model (8) produces fluctuations in density for $\beta \neq 0$ and $\epsilon > 0$. We use $\xi(x)$ to denote $\xi_t(x)$ given by (5) with $n_t(x)$ replaced by $n(x)$, and $\sigma^2(\xi(x))$ to denote $\sigma^2(\xi_t(x))$ given by (7) with $\xi_t(x)$ replaced by $\xi(x)$. $\xi(x)$ can be

viewed as a function of $n(x)$. The Laplace kernel $k(x-y,\sigma^2(\xi))$ takes the form of

$$k(x-y,\sigma^2(\xi(y))) = \frac{1}{\sqrt{2}\sigma(\xi(y))}e^{-\sqrt{2}|x-y|/\sigma(\xi(y))}.$$

Let

$$H(x-y,n(y)) = k(x-y,\sigma^2(\xi(n(y))))f(n(y)).$$

We use $(\frac{1}{\sigma(\xi(n))})'$ to denote the derivative of $\frac{1}{\sigma(\xi(n))}$ with respect to n, and $H'(x-y,n)$ to denote the partial derivatives of H with respect to n. Then

$$H'(x-y,n(y)) = k(x-y,\sigma^2(\xi(n(y))))f'(n(y))+$$

$$\frac{1}{\sqrt{2}}e^{-\sqrt{2}|x-y|/\sigma(\xi(n(y)))}[1-\frac{\sqrt{2}|x-y|}{\sigma(\xi(n(y)))}]f(n(y))(\frac{1}{\sigma(\xi(n))})'.$$

For $n(y) > n_{thresh}$, $f'(n(y)) = 0$. We therefore have that for $n(y) > n_{thresh}$,

$$H'(x-y,n(y)) = \frac{1}{\sqrt{2}}e^{-\sqrt{2}|x-y|/\sigma(\xi(n(y)))}[1-\frac{\sqrt{2}|x-y|}{\sigma(n(y))}]f(n(y))(\frac{1}{\sigma(\xi(n(y)))})'.$$

Since $\epsilon > 0$, for $n \neq n_{thresh}$, $\frac{d\xi(n)}{dn} > 0$, and $\frac{d\sigma(\xi)}{d\xi} > 0$ (< 0) if $\beta > 0$ $(\beta < 0)$. It follows that $(\frac{1}{\sigma(\xi(n))})' < 0 (> 0)$ if $\beta > 0$ $(\beta < 0)$.

If $\lambda = 0$, then $H(x-y,n(y))$ equals zero for $0 \leq n(y) < n_{thresh}$, has a jump at n_{thresh}, and then decreases in $n(y)$ in the interval $|x-y| < \sigma(\xi(n(y)))/\sqrt{2}$ when $\beta > 0$ or in the interval $|x-y| > \sigma(\xi(n(y)))/\sqrt{2}$ when $\beta < 0$.

If $\lambda > 0$, $H'(x-y,0) = k(x-y,\sigma^2(\xi(0)))f'(0) = k(x-y,\sigma^2(\xi(0)))\lambda > 0$. We have that $H(x-y,n(y))$ increases in $n(y)$ when $n(y)$ is small, and decreases in $n(y)$ in the interval $|x-y| < \sigma(\xi(n(y)))/\sqrt{2}$ when $\beta > 0$ or in the interval $|x-y| > \sigma(\xi(n(y)))/\sqrt{2}$ when $\beta < 0$.

We have proven that for positive ϵ and for $\lambda \geq 0$, $H(x-y,n(y))$ produces fluctuations in density in the interval $|x-y| < \sigma(\xi(n(y)))/\sqrt{2}$ when $\beta > 0$ or in the interval

523 $|x - y| > \sigma(\xi(n(y)))/\sqrt{2}$ when $\beta < 0$.